

Supplementary 3D PDF files (S1–S3) from synchrotron scan models are available linked to the online version of the paper.

Summary of available 3D data:

S1, Arm segments from *Ophiocoma wendtii*.

S2, Arm segments from *Ophiocoma echinata*.

S3, Arm segments from *Ophiocoma pumila*.

Scan data are available through Dryad at <https://doi.org/10.5061/dryad.kc041>

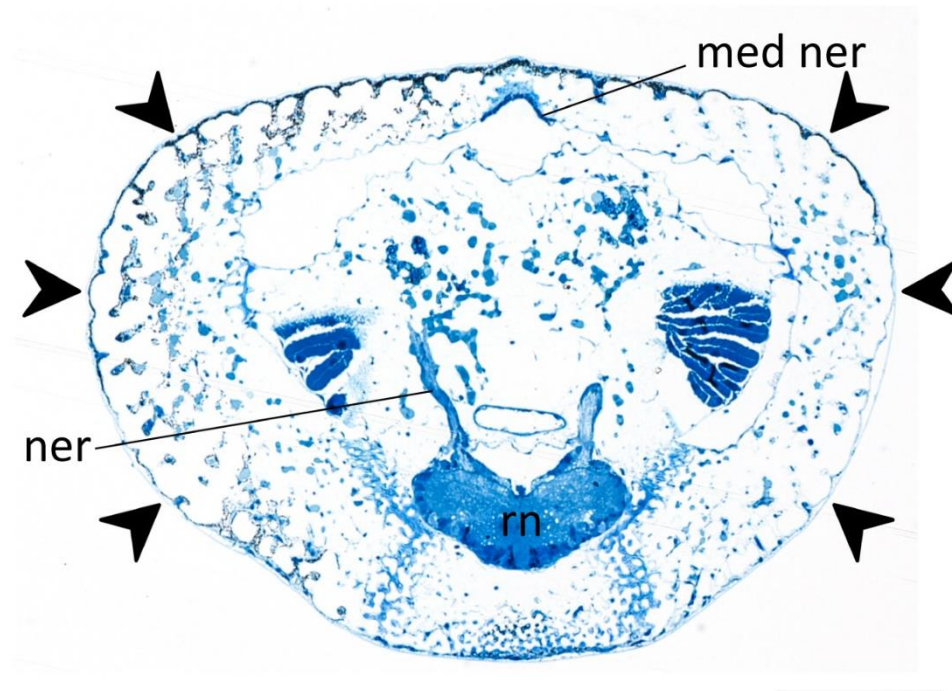


Figure S4. Innervation of the arm plates in *Ophiocoma wendtii*. The large radial nerve cord, runs along the centre of the oral (ventral) arm and emits paired nerves from the hyponeural part, which project aborally (dorsally). At the aboral (dorsal) side, a smaller median nerve cord is present directly beneath the dorsal arm plate. The median and radial nerve cords emit smaller nerves laterally and distally, which branch and project between the EPTs (examples indicated by arrowheads). EPTs are present in the lateral arm plates as well as the dorsal and ventral plates (see Figure 1). Scale bar, 500 μ m. Med ner, median nerve; ner, nerve bundles; rn, radial nerve.

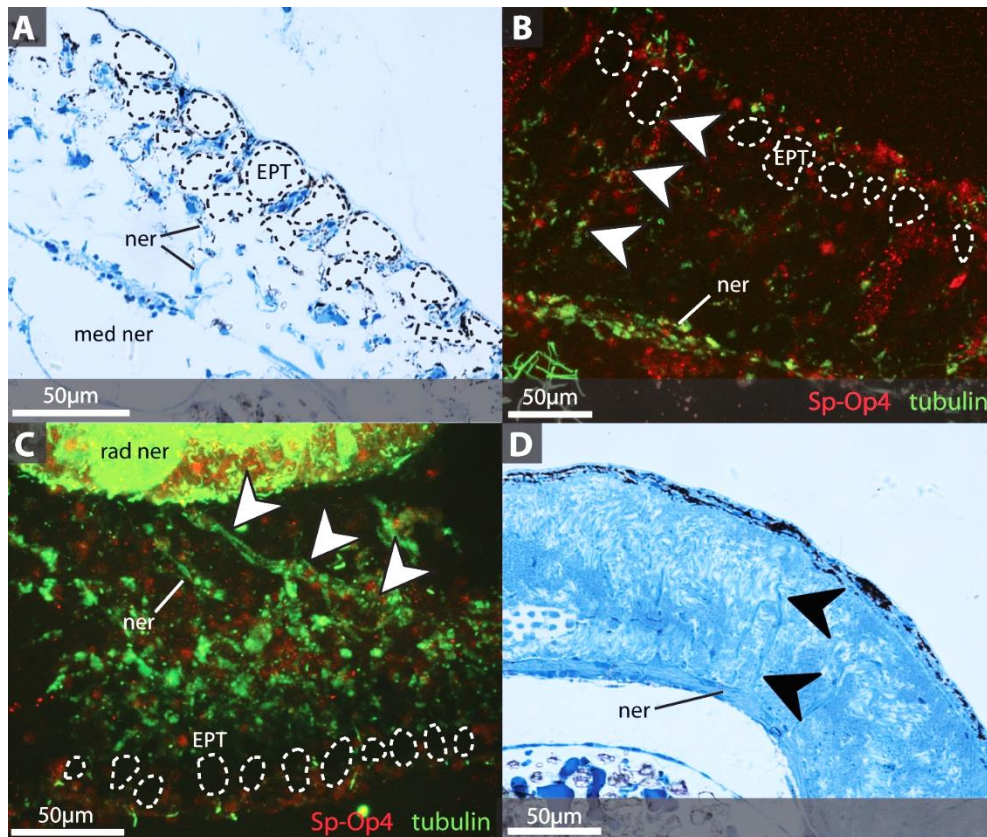


Figure S5. Arm plate innervation and opsin reactivity in *Ophiocoma echinata*. *Ophiocoma echinata* demonstrates a very similar arm plate innervation pattern to *O. wendtii* and *O. pumila* (Figures 3 and 4), with nerve bundles from the median and lateral nerves (A, B, D; arrowheads) and radial nerve cord (C, arrowheads) projecting between the EPTs towards Sp-Op4-reactive cells near the surface of the arm plates (B, C). Ciliary bundles are also present between the EPTs at the plate surface (B, C). Sp-Op4-reactive cells are also present in the outer soma of the radial nerve cord (C). In the medial part of the lateral arm plate, where EPTs are absent (D), nerve bundles are also seen projecting towards the surface from a nerve beneath the plate. All panels are transverse sections. EPT, expanded peripheral trabecula; med ner, median nerve; ner, nerve bundles; rad ner, radial nerve.

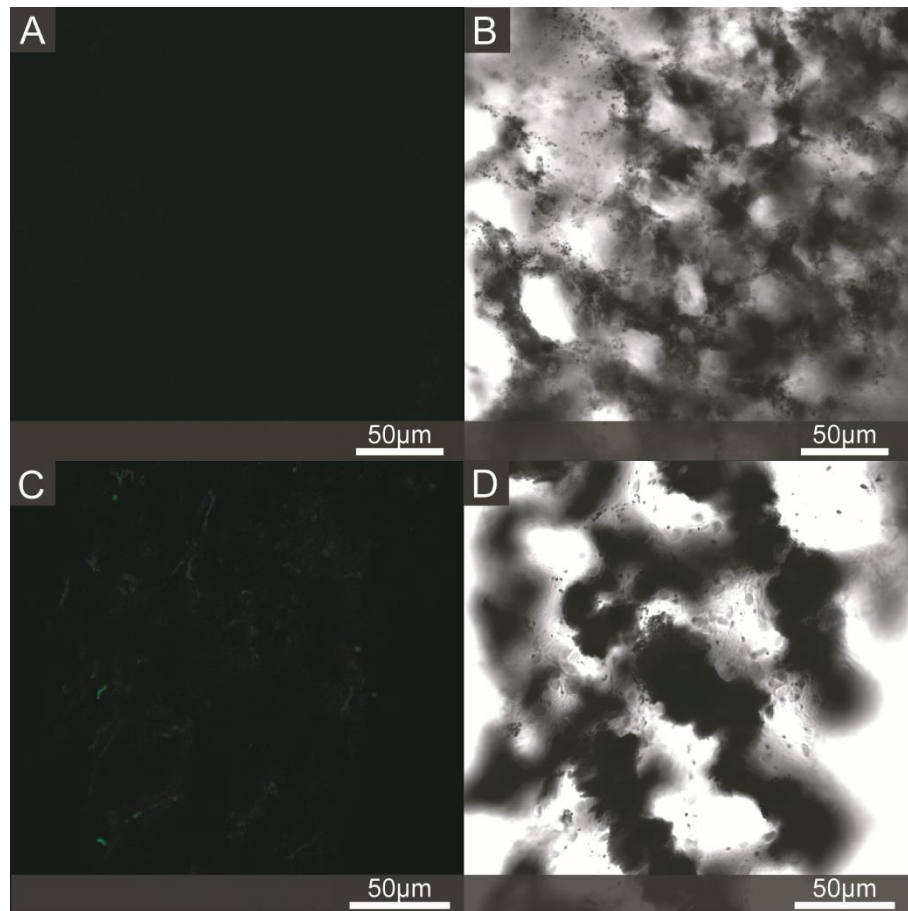


Figure S6. Control immunolabelling experiments. Dorsal arm plates of *Ophiocoma wendtii* were used in control experiments lacking antibodies to examine fluorescence (**A**, **B**), and lacking primary antibodies to test the activity of the secondary antibodies in the absence of a target (**C**, **D**). Left panels are composite images from three laser channels; right panels are transmission images.

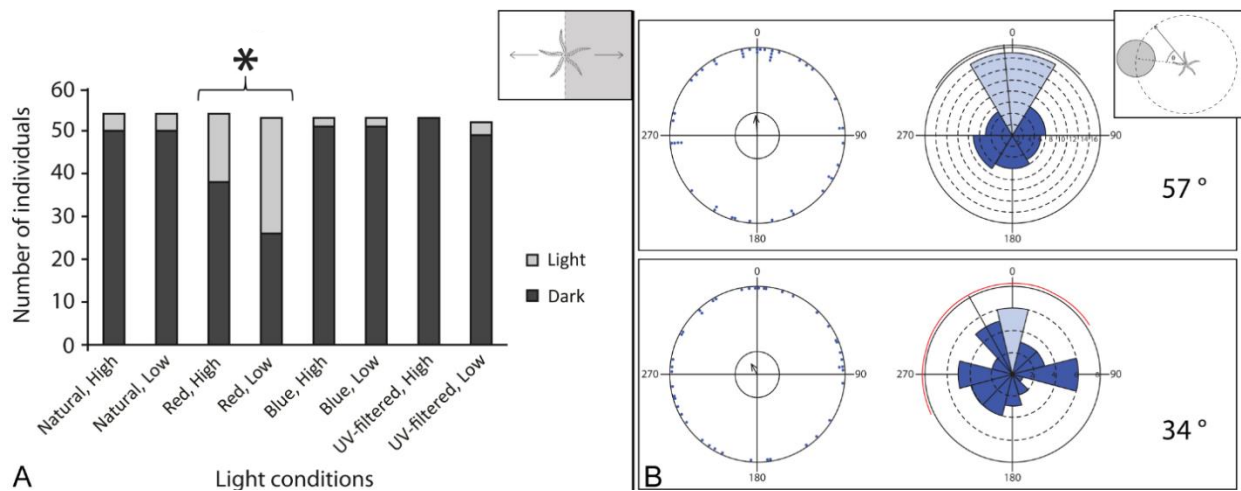


Figure S7. Photoresponses and behaviour in *Ophiocoma wendtii*. **A**, Results of light-dark choice experiments in *Ophiocoma wendtii*. Animals ($n = 55$) overwhelmingly chose the darkened tank area under natural, blue, and UV-filtered light, but not under red light (Fisher's Exact test, $p < 0.00001$, asterisk). There were no significant differences between high and low light intensity treatments (Fisher's Exact test, $p > 0.05$). **B**, Results of spatial resolution experiments. Left, raw data plots indicating exit bearings of all subjects relative to a shadow target ($n = 44$). Central arrow indicates mean vector, length approaching statistical significance at the 0.05 level (inner circle, Rayleigh test for uniformity). Right, rose histogram bars indicate frequency of subjects exiting the arena within the indicated bearing classes (class widths adjusted according to target size). Subjects successfully reaching the target are highlighted in pale blue. Solid black radius indicates mean exit vector, red arc indicates non-significant, and black arc indicates statistically significant 95% confidence interval for mean exit vectors. Target position is corrected to 0° throughout.

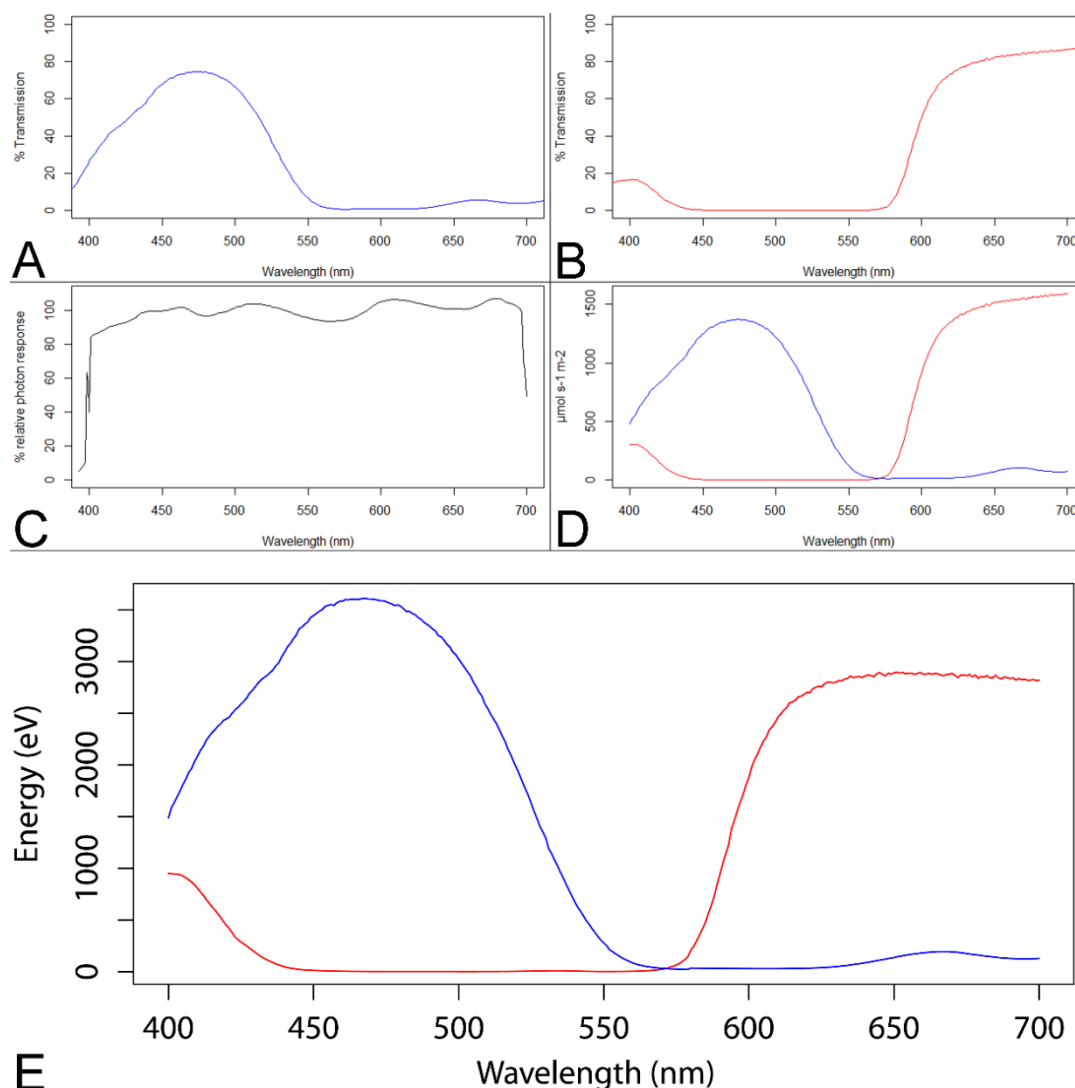


Figure S8. Filter spectra, spectral response, and light energy. **A, B,** Transmission spectra of blue (**A**) and red (**B**) filters. **C,** Spectral response curve for LICOR LI-192 PAR meter. **D,** Filter spectra corrected to account for spectral response of PAR meter (Table S9). Note the minimal overlap between spectra. Total number of photons transmitted under red filter (area beneath spectrum) is 6% greater than under the blue filter in constant intensity daylight. **E,** Energy received beneath each filter in high intensity daylight ($300,000 \mu\text{mol s}^{-1} \text{m}^{-2}$). Total energy under blue filter (area beneath spectrum) is 23% greater than under the red filter. However, differences in behaviour are not solely attributable to this, as evidenced by the absence of response to high intensity red light (total est. energy 318,292 eV) but the presence of a response to low-intensity blue light (total est. energy 159,290 eV).

Table S9. Sample calculations for photon numbers and energy, under the red filter at wavelengths 400–410 nm (Figure S7).

Wavelength (nm)	Filter trans- mission (%)	PAR spectral response (%)	Total detection (%) [§]	Prop. of total light detected (%) [⌘]	Photons ($\mu\text{mol m}^{-2} \text{ s}^{-1}$) [†]	Energy per photon (eV)	Total energy (eV)
400	16.62	39.97	6.64	0.074	306.504	3.0995	950.01
401	16.63	84.45	14.04	0.157	306.698	3.0918	948.24
402	16.59	85.07	14.11	0.158	306.032	3.0840	943.83
403	16.65	85.46	14.23	0.159	307.050	3.0764	944.62
404	16.57	85.94	14.24	0.159	305.591	3.0688	937.80
405	16.39	86.42	14.16	0.158	302.191	3.0612	925.08
406	16.14	86.81	14.01	0.157	297.68	3.0537	909.02
407	15.80	87.27	13.79	0.154	291.445	3.0462	887.80
408	15.49	87.69	13.58	0.152	285.617	3.0387	867.91
409	15.00	88.17	13.23	0.148	276.719	3.0313	838.82
410	14.47	88.56	12.82	0.143	266.894	3.0239	807.06

[§] Product of filter transmission and spectral response to give % detection by PAR meter.

[⌘] Proportion of total light detected falling within this wavelength class, as a percentage.

[†] Total intensity of photons within this wavelength class (of a total 165,000 $\mu\text{mol m}^{-2} \text{ s}^{-1}$ as detected under red filter) corrected for the bias in spectral response by PAR meter:

$$\frac{\text{Proportion of total light detected} \times 165,000 \mu\text{mol m}^{-2} \text{ s}^{-1}}{\text{Spectral response}}$$

Supplemental data: Behavioural experiments

Methods

It has been demonstrated that light spectra and polarization affect photoresponsive behaviours in other ophiuroids [S1,S2,11], but these factors remain to be thoroughly investigated in *O. wendtii*. Despite repeated references to their ability to identify and move towards targets on a horizon [7,9], this has never been rigorously tested. We conducted some preliminary investigations into basic light-responsive behaviour in *Ophiocoma*.

To test overall light sensitivity in *Ophiocoma wendtii*, specimens were placed at the centre of a tank (35 cm x 42 cm, depth 30 cm) which was half illuminated and half shaded using black sticky-backed plastic (Figure S7A). The subjects' movements and time taken to establish direction were recorded, and if there was no movement after 60 s trials were stopped. The illumination of the arena was manipulated in spectrum using a variety of coloured plastics. Full-spectrum, UV-filtered, red (peak $\lambda = 700$ nm, see Figure S8) and blue (peak $\lambda = 475$ nm, see Figure S8) lights were used, each at a slightly higher and a lower intensity, giving a total of eight treatments. Filter transmission spectra were measured using a Helios Beta spectrophotometer (Thermo Scientific). The blue filter gave peak transmission (76%) at 475 nm; width at half maximum transmission was 115 nm. The red filter gave peak transmission (86%) at 700 nm; width at half maximum was 102 nm (within visible range up to 700 nm). Individuals ($n = 55$) were tested twice daily under different treatments until each had experienced all treatments in a randomised order. Tanks were cleaned, refilled, and reoriented between trials to exclude conspecific chemical cues, temperature gradients caused by shading, and magnetic field direction.

To assess potential for basic spatial resolution in *Ophiocoma wendtii*, specimens ($n = 44$) were placed at the centre of a circular arena (diameter 0.6 m or 1 metre, depth 30 cm) with a round black shade target (diameter 30 cm) suspended at a randomised point on the edge of the arena (Figure S7B), and their movement was monitored over five minutes. The shade occupied 57° of the horizon in the 0.6 m arena and 34° in the 1 metre arena. Two metrics were measured: the direction in which the subject exited the arena as a bearing relative to the target, and whether or not the subject moved directly under the shade (i.e. the disk moved across the arena boundary within the shadow cast by the target). Data were analysed in Oriana 4 (Kovach Computing Services) to test for departure from uniformity (Rayleigh test, V test), and to calculate confidence intervals for the mean bearing in each treatment. Success/failure scores were analyzed using Bernoulli trial binomial statistics in R [S3]. All behavioural experiments were performed in outdoor aquaria supplied with fresh seawater, at the Smithsonian Tropical Research Institute in Bocas del Toro, Panama, during February–April 2015.

Basic comparative light intensity measurements were taken using a LI-192 underwater PAR quantum sensor with LI-250 handheld meter (optimised for near-uniform sensitivity across 400–700 nm, see SM2, LI-COR Biosciences). In light-dark choice arenas, high intensity light treatments fell within a range of 250,000–330,000 $\mu\text{mol s}^{-1} \text{m}^{-2}$ and low intensity between 50,000–125,000 $\mu\text{mol s}^{-1} \text{m}^{-2}$. The red filter allowed 54%, the blue filter 51%, and the UV filter 90% visible light transmission (by number of photons in $\mu\text{mol s}^{-1} \text{m}^{-2}$ after accounting for differential spectral response in the PAR meter, see Figure S8 and Table S9). Total light energy available under the red filter was 25.1% lower than under the blue filter (see Figure S8 and Table S9); the inclusion of two overall light intensity levels aimed to remove this as a confounding factor. Light intensity in shaded halves of the tanks was generally around 35% of that in the illuminated halves. In spatial resolution experiments, light intensity beneath the target was less than half that at the centre of the arena (126,500 $\mu\text{mol s}^{-1} \text{m}^{-2}$ beneath target, 275,000 $\mu\text{mol s}^{-1} \text{m}^{-2}$ at centre). The light intensities in high intensity treatments and at the centre of the arena were comparable to that measured at a depth of 25 cm in local reef (327,000 $\mu\text{mol s}^{-1} \text{m}^{-2}$). See Figure S8 and Table S9 for full details of spectra and corrections for spectral sensitivity of PAR meter.

Results

Ophiocoma wendtii overwhelmingly (means 92–100%) preferred shaded areas to lit ones under full-spectrum, blue, and UV-filtered light conditions (Figure S7). Under red light, significantly more subjects entered the lit areas than under any of the other light spectra (Fisher's Exact Test, $p < 0.0001$; Figure S6). There were no significant differences between the slightly higher and lower intensities (Fisher's Exact Test, $p > 0.05$), and when intensities are pooled red light still elicited significantly different responses to all other spectra (Fisher's Exact Test, $p < 0.0001$). Subjects made a 'choice' within the minute allowed in 96% of trials, with most trials (58%) lasting 5 s or less. A small amount of short-wavelength light transmitted by the red filter (400–425 nm, Figure S8) did not recover negative photoresponsive behaviour; we anticipate that peak sensitivity lies between 450–550 nm.

In target-seeking experiments, subject orientation was skewed significantly towards the centre of targets occupying 57° of the horizon (mean bearing $\mu = 354.6^\circ$ where target position is corrected to $0^\circ/360^\circ$, r vector length 0.221; V test, $u = 2.061$, $p = 0.019$; Figure S6). This was not detected by the less powerful Rayleigh test ($Z = 2.144$, $p = 0.117$); the V test accounts for the *a priori* known position of the target [S4]. Subjects presented with a target occupying 33° of the horizon did not orient differently from random (mean bearing $\mu = 330.8^\circ$, r vector length 0.138; V test, $u = 1.127$, $p = 0.131$; Rayleigh test, $Z = 0.833$, $p = 0.437$; Figure S6). The number of individuals that located the target successfully was significantly higher than random with a 57° target (Bernoulli trial, $p = 0.029$), but not a 33° target ($p = 0.058$). Animals responded quickly, with 50% reaching the edge of the arena in 10 s or less and no individual taking more than 23 s. Subjects rarely changed direction and usually maintained a distinct bearing throughout.

References

- S1. Johnsen S. 1994 Extraocular sensitivity to polarised light in an echinoderm. *J. Exp. Biol.* **195**, 281–291.
- S2. Johnsen S, Kier WM. 1999 Shade-seeking behaviour under polarized light by the brittlestar *Ophioderma brevispinum* (Echinodermata: Ophiuroidea). *J. Mar. Biol. Assoc. UK* **79**, 761–763. (doi:10.1017/S0025315498000940)
- S3. R Development Core Team. 2014 R: A language and environment for statistical computing.
- S4. Durand D, Greenwood JA. 1958 Modifications of the Rayleigh test for uniformity in analysis of two-dimensional orientation data. *J. Geol.* **66**, 229–238.